JETIR.ORG ISSN: 2349-5162 | ESTD Year : 2014 | Monthly Issue
JOURNAL OF EMERGING TECHNOLOGIES AND INNOVATIVE RESEARCH (JETIR)
An International Scholarly Open Access, Peer-reviewed, Refereed Journal

DARCY-FORCHHEIMER MHD FLOW OF POWER-LAW FLUID MODEL WITH JOULE HEATING, HEAT SOURCE, AND VISCOUS DISSIPATION

Mira Das[1] and Utpal Jyoti Das[2]
[1]Assistant Professor of Mathematics.
[2]Assistant Professor of Mathematics.
[1]Department of Mathematics,Mahapurusha Srimanta Sankaradeva Viswavidyalaya, Nagaon, Assam, India
[2]Department of Mathematics, Gauhati University, Assam, Guwahati-781014, India.

1. ABSTRACT:

An analysis of MHD power-law fluid over a stretching/ shrinking surface in a non-linear Darcy-Forchheimer porous medium has been considered. The study includes the influence of Joule heating, viscous dissipation and heat source. The MATLAB in built bvp4c method has been used for the solution of the consequential non-linear differential equations. Influence of relevant physical parameters on velocity, temperature distribution and skin friction are discussed for pseudoplastic and dilatant fluid. It is noticed that the local Forchheimer parameter and power-law parameter helps to reduce the fluid velocity, while Eckert number raises the fluid velocity. Also, decrease in rate of strain is seen when the values of power-law parameter, local Forchheimer parameter and stretching parameter enhances in the pseudoplastic and dilatant fluid.

Keywords: bvp4c; Darcy-Forchheimer; Power-law fluid; stretching surface; viscous dissipation.

2. NOMENCLATURE:

A	Energy dissipation parameter
B_0	Strength of the magnetic field
C_k	Drag coefficient
d	Stretching/shrinking rate
E	Eckert number
G	Local Forchheimer number
h	Strength of stagnation flow

H Magnetic field parameter
K Porous parameter
K_1 Consistency coefficient
K_p Permeability of the porous medium
m Stretching parameter
n Power-law index
N Power-law parameter
Pr Prandtl number
Q Heat source parameter
T Fluid temperature
T_w Stretching sheet temperature
T_∞ Ambient temperature
u Velocity in x-direction
u_e Speed of external flow
u_s Speed of stretching sheet
v Velocity component in y-direction
(x, y) Cartesian co-ordinates

Greek symbols

α Thermal diffusivity
μ Coefficient of viscosity
θ Non-dimensional parameter
ρ Fluid density
σ Electrical conductivity
υ Kinematic viscosity
ψ Stream function

3. INTRODUCTION

The study of magnetohydrdynamic flow of non-Newtonian fluid over a stretched surface has a great significance owing to its wide applications in engineering. Also, the shrinking effect plays an essential role, as this effect has reverse flow and has been found to be important in the polymer and textile industries. Mahapatra et al. [1] studied magnetohydrodynamic power-law fluid model in a stretching sheet near stagnation point. Dash et al. [2] analyzed the boundary layer stagnation point flow in a stretching/shrinking sheet. Also, several authors have reported the rheological property of non-Newtonian fluids over stretched/ shrinking surface. Some of them are [3-15].

In heat transfer analysis, dissipation effects play the role of internal energy source. The Joule heating and viscous dissipation effects are more significant while the plate is heated or cooled. The observed fact of heat transfer typically occurs in microchip processes, power generation systems, and nuclear reactor cooling. Kumar et al. [16] presented the impact of viscous dissipation and Joule heating on Oldroyd B fluid flow in stretching sheet using shooting algorithm with RKF45 method. Das [17] studied the viscous dissipation and Joule heating effects on Cason fluid model with non-uniform magnetic field using bvp4c method. Rasheed et al [18] presented Jeffrey nano-fluid flow in a stretchable cylinder incorporating viscous dissipation and Joule heating property.

The application of fluid flow through porous media can be observed in diversified fields such as nuclear engineering, geothermal physics. Darcy's law is commonly used to elucidate the flow that fills pores. Darcy's law is not valid for the effects of high velocity and turbulence in the pore space. Forchheimer [19]

introduced the quadratic polynomial into the momentum equation to estimate the impact of inertia on visible permeability. Several studies have examined the flow in porous medium using the Darcy-Forchheimer model with various geometries. Some have been reported here. Sadiq and Hayat [20] presented Maxwell fluid flow with the Darcy-Forchheimer model over a surface. Seth et al. [21] studied the Darcy-Forchheimer flow model over an inclined stretching sheet including Soret with Dufour effects. Recently, Rasool et al. [22], Mishra et al. [23], Hayat et al. [24], Saeed et al. [25], and Ullah [26] studied the Darcy-Forchheimer flow model over stretched surface.

In this study, Darcy-Forchhemier MHD flow model of power-law fluid in a stretching/shrinking sheet incorporating Joule heating, heat source and viscous dissipation is addressed.

2. MATHEMATICAL FORMULATION

Consider a steady, incompressible MHD flow of power-law fluid around a stagnation point over a stretched plate surrounded in a Darcy-Forchheimer porous medium. The x- axis is considered along the surface originating from the stagnation point and the y- axis perpendicular to it (Fig.1). The speed of the stretching sheet is assumed as $u = u_s(x) = dx$ and speed of external flow is $u = u_e(x) = hx.$

The governing boundary layer equations incorporating heat source, Joule heating and viscous dissipation (Choudhary et al. [3], Dey and Mahanta [15], Misra et al. [23]) are

$$\frac{\partial u}{\partial x}+\frac{\partial v}{\partial y}=0 \tag{1}$$

$$u\frac{\partial u}{\partial x}+v\frac{\partial u}{\partial y}=u_e\frac{du_e}{dx}+\upsilon\frac{\partial^2 u}{\partial y^2}+\frac{K_1}{\rho}\frac{\partial}{\partial y}\left(\frac{\partial u}{\partial y}\right)^n-\frac{C_k}{\sqrt{K_p}}(u_e-u)^2+\left(\frac{\upsilon}{K_p}+\frac{\sigma B_0^2}{\rho}\right)(u_e-u) \tag{2}$$

$$u\frac{\partial T}{\partial x}+v\frac{\partial T}{\partial y}=\alpha\frac{\partial^2 T}{\partial y^2}+\frac{\sigma B_0^2}{\rho}(u_e-u)^2+\frac{\mu}{\rho C_p}\left(\frac{\partial u}{\partial y}\right)^{n+1}+\frac{Q_0}{\rho C_p}(T-T_\infty) \tag{3}$$

with conditions

$$u=u_s=dx, v=0, T=T_w \text{ at } y=0; \qquad u=u_e=hx,\ T\to T_\infty \text{ as } y\to\infty. \tag{4}$$

Following similarity variables are used

$$\psi=\sqrt{h\alpha x}\, f(\eta), \eta=y\sqrt{\frac{h}{\alpha}}, \theta=\frac{T-T_\infty}{T_w-T_\infty}, \tag{5}$$

where stream function (ψ) is

$$u=\frac{\partial\psi}{\partial y}, v=-\frac{\partial\psi}{\partial x}.$$

Using (5) in (1)-(3), reduces to the following dimensionless equations

$$\Pr g'''-g'^2+gg''+(K+H)(1-g')+Ng'''g''^{(n-1)}-G(1-g'^2)+1=0, \tag{6}$$

$$\theta''+g\theta'+Q\theta+Ag''^{(n+1)}+HE(1-g')^2=0, \tag{7}$$

with

$$g=0, g'=\frac{d}{h}=m, \theta=1 \text{ at } \eta=0;\ g'\to 1, \theta\to 0 \text{ as } \eta\to\infty, \tag{8}$$

where prime is used for differentiation with respect to η ,

$$\Pr=\frac{\upsilon}{\alpha}, H=\frac{\sigma_e B_0^2}{h\rho}, K=\frac{\upsilon}{hK_p}, Q=\frac{Q_0}{h\rho C_p},\ E=\frac{u_e^2}{C_p(T_w-T_\infty)}, A=\frac{\mu a^{1/2}}{\rho C_p\alpha^{1/2}(T_w-T_\infty)}, G=\frac{C_k x}{\sqrt{K_p}},.$$

$$N = \frac{nK_1 x^{n-1} a^{\frac{3}{2}(n-1)}}{\rho \alpha^{\frac{1}{2}(n+1)}}.$$

Here, m represent stretching parameter when $m > 0$ and shrinking parameter when $m < 0$.

3. METHOD OF SOLUTION

The equations (6) and (7) are coupled non-linear, so the solution in closed form is not possible.
Setting $f = z_1, f' = z_2, f'' = z_3, \theta = z_4, \theta' = z_5$, the equations (6) - (7) transform to the following first order ordinary differential equations

$$z_5' = -z_1 z_5 - A z_3^{n+1} - HE(1 - z_2)^2 - Q z_4, \tag{9}$$

$$(\Pr + N z_3^{n-1}) z_3' = z_2^2 - z_1 z_3 - (K + H)(1 - z_2) + G(1 - z_2)^2 \tag{10}$$

with boundary conditions

$$z_1(0) = 0, z_2(0) = m, z_4(0) = 1;\ z_1(1) = 1, z_4(1) = 0. \tag{11}$$

The bvp4c method is applied for the solution of Eqs. (9)-(10) subject to (11).

4. RESULTS AND DISCUSSION

In this section, the influence of local Forchheimer parameter (G), magnetic field parameter (H), power-law parameter (N), stretching/ shrinking parameter (m) on velocity and the impact of local Forchheimer parameter, heat source parameter (Q), Eckert number (E) on temperature are discussed. Also, the effect of related parameters on skin friction is analyzed. Following default values are taken for computation:

$$H = 0.5, K = 0.5, E = 0.5, m = 0.2, \Pr = 2,\ \Pr = 2, N = 0.5, A = 0.5, G = 0.5, Q = 0.5.$$

Figures 2 and 3 represent the variation of $g'(\eta)$ against η for different values of G with $n = 0.5$ and $n = 1.5$, respectively. Figure 2 depict that the local Forchheimer number lowers the movement of fluid particles for pseudoplastic $(n = 0.5 < 1)$ fluid and the same behaviour of fluid particles is seen from figure 3 for dilatant $(n = 1.5 > 1)$ fluid.

Figures 4 -5 represents the impact of H on velocity $g'(\eta)$ for pseudoplastic $(n = 0.5 < 1)$ and dilatant fluid $(n = 1.5 > 1)$, respectively. Figures show that an increasing magnetic field parameter reduces the speed of fluid particles for both pseudoplastic $(n = 0.5 < 1)$ and dilatant fluid $(n = 1.5 > 1)$. Physically, increasing magnetic field parameter raises the resisting Lorentz force and thus reduces the speed of the fluid particles for both pseudoplastic and dilatant fluid.

Figures 6-7 shows the influence of power-law parameter (N) on $g'(\eta)$ for pseudoplastic $(n = 0.5 < 1)$ and dilatant fluid $(n = 1.5 > 1)$, respectively. It is observed that the velocity $f'(\eta)$ retards in both the cases due to increase in N.

Figures 8-9 represents the influence of stretching/ shrinking parameter (m) on velocity profile. For stretching sheet $m > 0$ and for shrinking sheet $m < 0$. $m = 0$ corresponds to stagnation point flow. It is seen that velocity profile accelerated as the parameter m rises. Thus, the thickness of the boundary layer flow increases for stretched sheet in comparison to shrinking or stagnation point flow.

Figures 10-11 represents the temperature curves against η when $n(= 0.5) < 1$ and $n(= 1.5) > 1$, respectively for various values of local Forchheimer parameter $(G = 0, 1, 2)$. In both the pseudoplastic $(n = 0.5 < 1)$ and dilatant

$(n = 1.5 > 1)$ cases the thermal boundary layer enhances faintly with the rising values of local Forchheimer parameter G.

Figures 12-13 represents the temperature curve against η when $n(= 0.5) < 1$ and $n(= 1.5) > 1$, respectively for various values of $Q(= 0.2, 0.6, 1)$. It shows an enhancement in thermal boundary layer due to the introduction of heat source parameter in both pseudoplastic and dilatant fluid. This is due to the fact that the presence of heat source transfers heat or energy to the flow, this energy contributes to improving the thermal boundary layer.

Figures 14-15 represents the temperature variation against η for different Eckert number $(E = 0, 1, 2)$ for pseudoplastic $(n = 0.5 < 1)$ and dilatant $(n = 1.5 > 1)$ fluid. It is observed that E enhances the thermal boundary layer thickness in both the cases of $n < 1$ and $n > 1$. It is entirely consistent with the present model which includes the energy loss due to Joule heating. The loss of energy led to an increase in the thickness of the thermal boundary layer Table 1 shows the skin friction $g''(0)$ for $n(= 1.5) > 1$ and $(n = 0.5) < 1$ across the surface for different values of N, G, H, m, K. The flow is not disturbed when the skin friction or gradient of fluid velocity is zero and as the values increase, a variation in the displacement of the flow is observed. Physically, gradient of fluid velocity or skin friction represent the strain rate per unit area. Thus, from Table 1, we can see that the strain rate increases when magnetic parameter (H) and permeability parameter (K) increases. But decrease in rate of strain is seen when the values of power-law parameter (N), local Forchheimer parameter (G) and stretching parameter (m) rises for both $n > 1$ and $n < 1$.

5. VALIDITY AND ACCURACY

The present study is well validated through the following investigations:

(i) When $n = 1, N = 0, G = 0, Q = 0, A = 0, E = 0,$ the present study matched with that of Chaudhary et al. [3].

(ii) When $E = 0, G = 0, Q = 0,$ the present study matched with that of Dey and Mahanta [15]

The comparison of the present study for $g''(0)$ with Chaudhary et al. [3] is presented in Table 2. It is found that the present result is in good agreement.

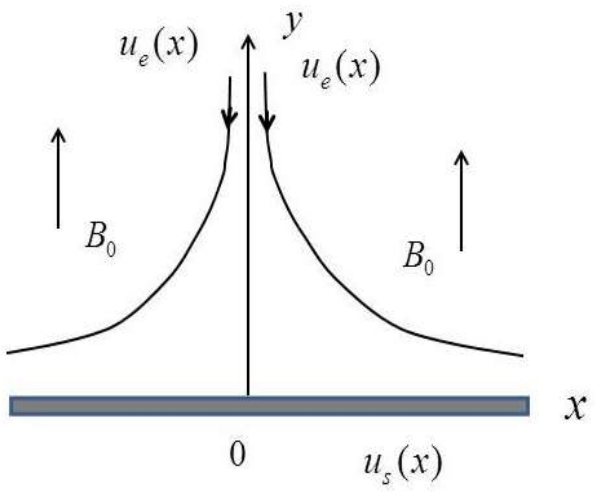

Figure1 Physical configuration.

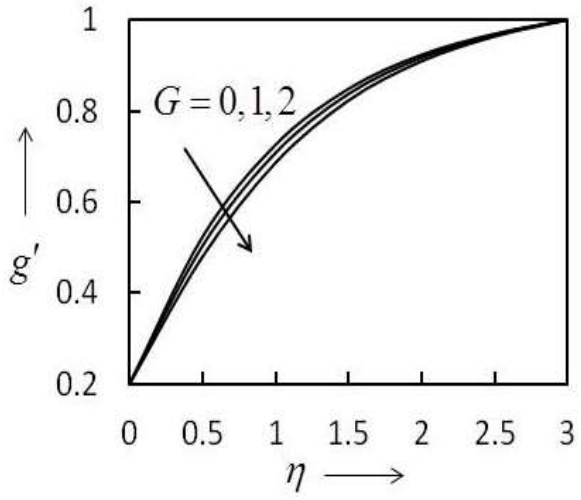

Figure 2 Influence of G on g' with n=0.5.

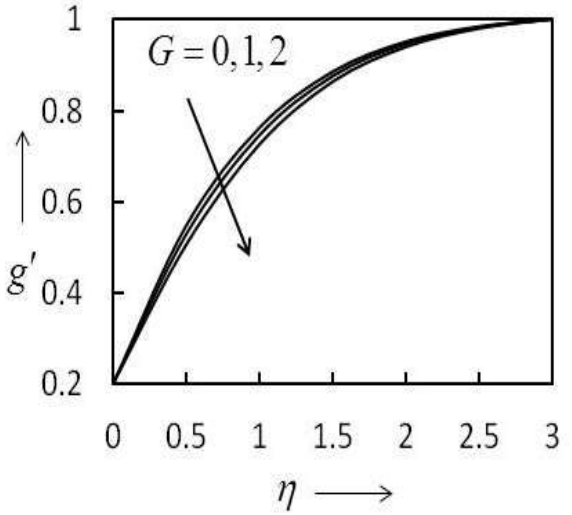

Figure 3 Influence of G on g' with n=1.5

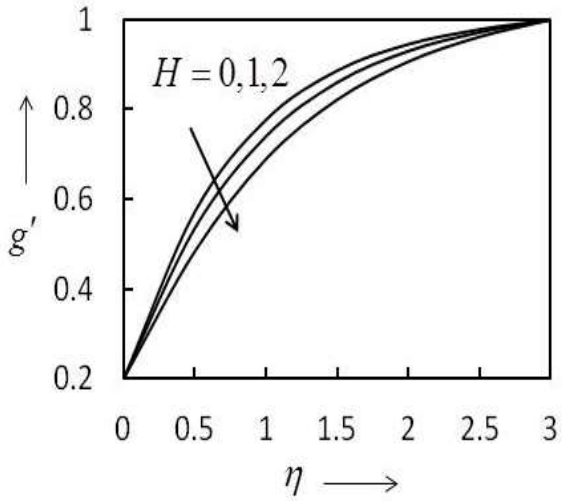

Figure 4 Influence of H on g' with n=0.

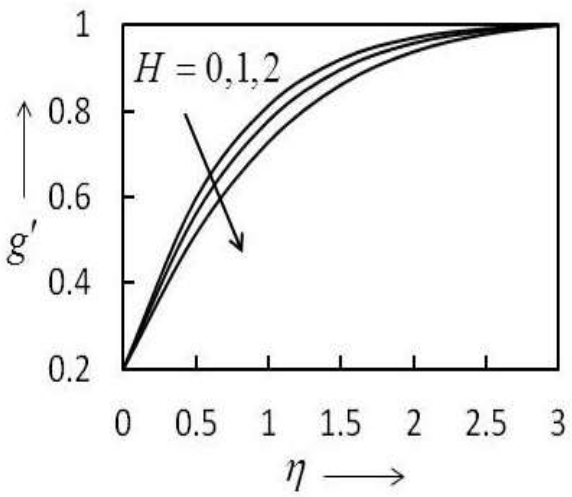

Figure 5 Influence of H on g' with n=1.5.

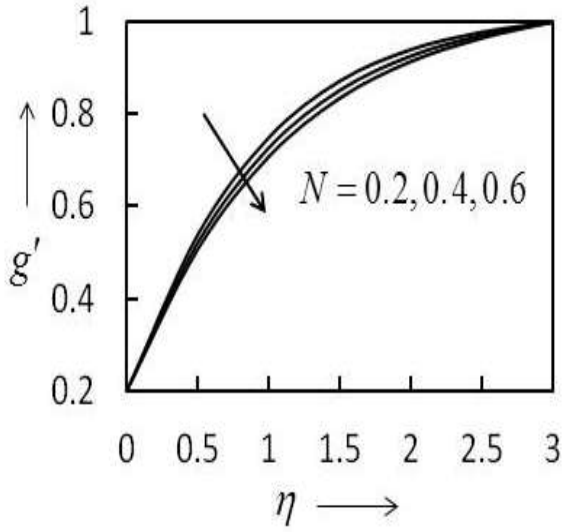

Figure 6 Influence of N on g' with n=0.5

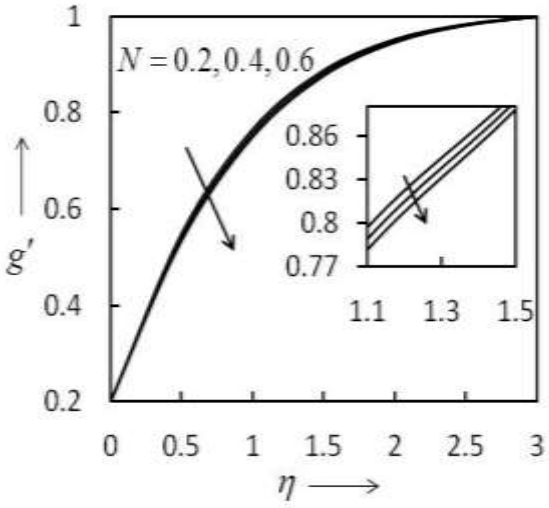

Figure 7 Influence N on g' with n=1.5.

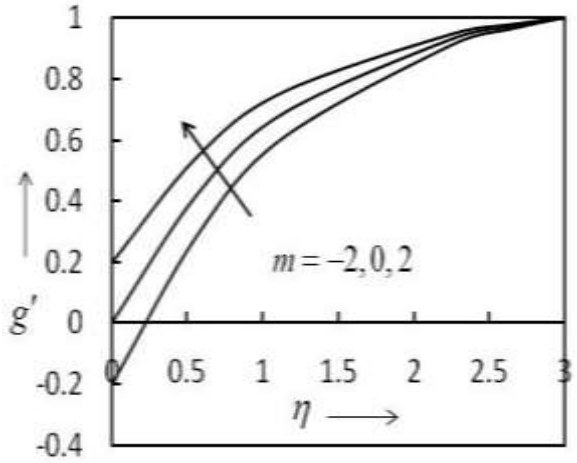

Figure 8 Influence of m on g' with n=0.5.

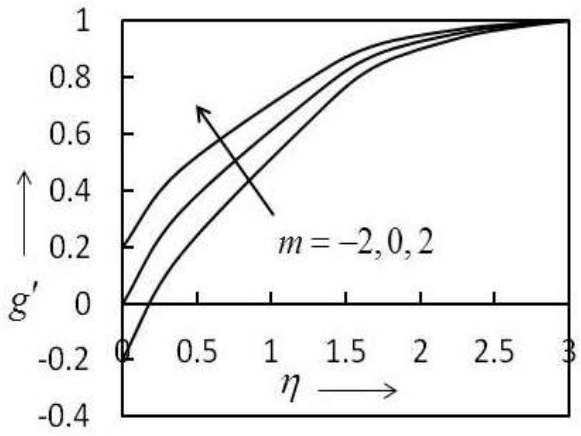

Figure 9 Influence of m on g' with n=1.5.

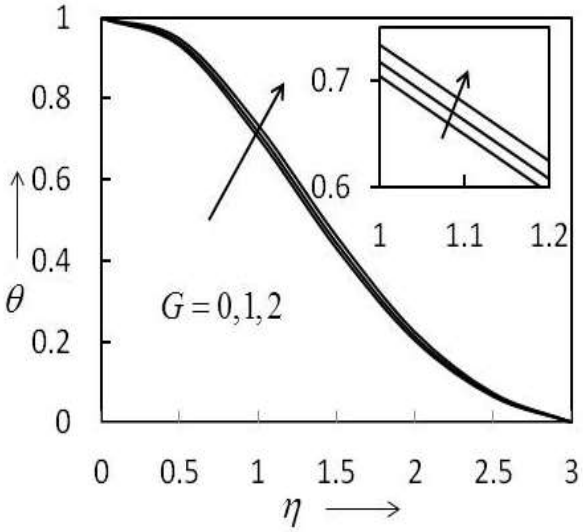

Figure 10 Influence of G on θ with n=0.5.

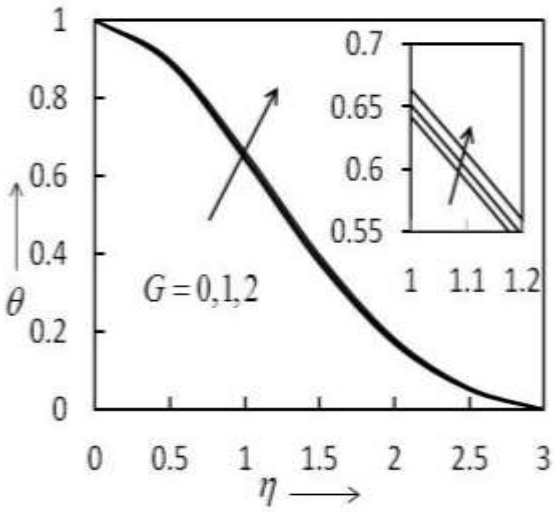

Figure 11 Influence of G on θ with n=1.5.

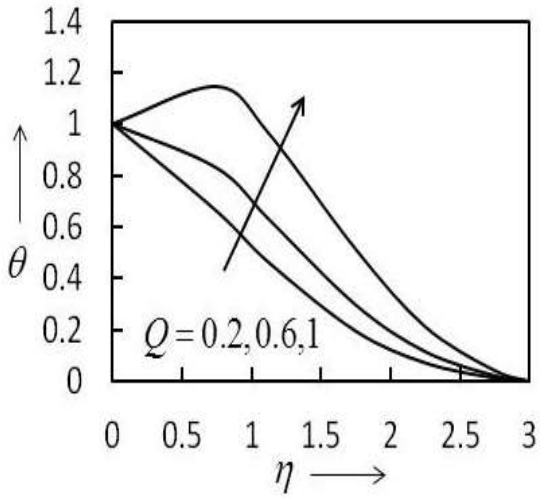

Figure 12 Influence of Q on θ with n=0.5.

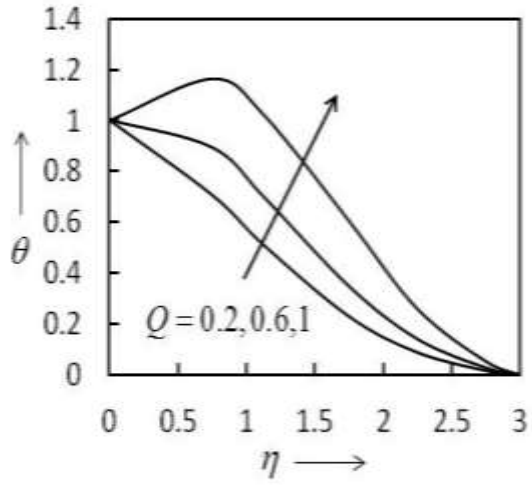

Figure 13 Influence of Q on θ with n=1.5.

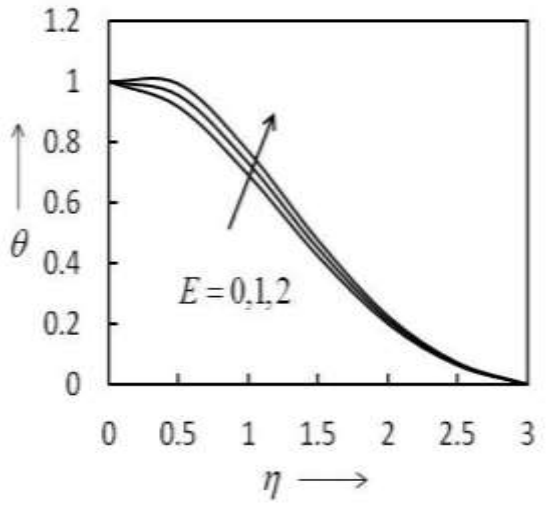

Figure14 Influence of E on θ with n=0.5.

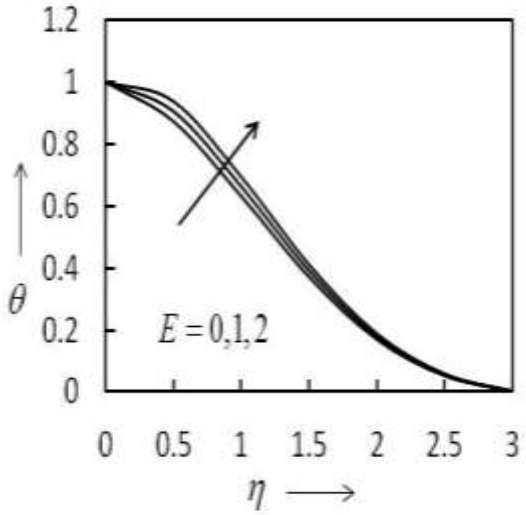

Figure 15 Influence of E on θ with n=1.5.

Tables:

Table1: Computational values of $g''(0)$.

N	G	H	m	K	$g''(0)$ $(n=1.5)$	$g''(0)$ $(n=0.5)$
0.5	0.5	0.5	0.2	0.5	0.8173	0.7587
0.3					0.8426	0.8041
0.1					0.8713	0.8572
	0.3				0.8340	0.7757
	0.1				0.8502	0.7923
		0.3			0.7851	0.7263
		0.1			0.7516	0.6929
			0.4		0.6511	0.5883
			0.6		0.4601	0.3986
				0.3	0.7851	0.7263
				0.1	0.7516	0.6929

Table2: Computation values of $g''(0)$ for Newtonian fluid $(n=1)$

$N=0, G=0, Q=0, A=0, E=0.$

Pr	K	H	m	$g''(0)$ (Chaudhary et al. (2016))	$g''(0)$ (Present study)
0.7	0.1	0.1	−0.1	1.67031	1.66431
1	0.1	0.1	−0.1	1.39749	1.39216
1	1	0.1	−0.1	1.74282	1.74098
1	0.1	3	−0.1	2.33510	2.32551
1	0.1	0.1	0.5	0.74709	0.74618

5. CONCLUSION

Main observations of the above study for pseudo plastic and dilatant fluid are as follows:

(i) Forchheimer number, magnetic field parameter, power-law parameter retards the fluid velocity.
(ii) Fluid velocity accelerated for higher stretching parameter.
(iii) The higher temperature is noted for larger values of local Forchheimer parameter, heat source parameter, Eckert number.
(iv) Skin friction is an increasing function of magnetic parameter and permeability parameter.
(v) Skin friction reduces for power-law parameter, local Forchheimer parameter and stretching parameter.

Competing Interests: There are no relevant financial or non-financial competing interests to report.

6. REFERENCES

[1] Mahapatra TR, Nandy SK, Gupta AS. Magnetohydrodynamic stagnation point flow of a power-law fluid towards a stretching surface. *Int J Non-Linear Mech*. 2009; 44: 124-129.
[2] Dash GC, Tripathy RS, Rashidi MM, Mishra SR. Numerical approach to boundary layer stagnation-point flow past a stretching/shrinking sheet. *J Mol Liq*. 2016; 221: 860-866.
[3] Chaudhary S, Singh S, Chaudhary S. Numerical solution for magnetohydrodynamic stagnation point flow towards a stretching or shrinking surface in a saturated porous medium. *Int J Pure Appl Math*. 2016; 106: 141-155.
[4] Gireesha BJ, Archana M, Prasannakumara BC, Gorla, RSR, Makinde, OD. MHD three dimensional double diffusive flow of Cassonananofluid with buoyancy forces and nonlinear thermal radiation over a stretching surface. *Int J Numer Method Heat Fluid Flow*. 2017; 27(12): 2858-2878.
[5] Mahantesh MN, Vajeravelu K, Abel MS, Siddalingappa MN. MHD flow and heat transfer over a stretching surface with variable thermal conductivity and partial slip. *Meccanica*. 2017; 48(6): 1451-1464.
[6] Alladin N, Bachok N, Nasir N. Effect of thermal radiation on MHD stagnation point flow over a shrinking sheet. *Journal of Physics Conference Series*. 2019; 1366: 012050.
[7] Yang M, Lin Y. Flow and heat transfer of non-Newtonian Power law fluids over a stretching surface with variable thermal conductivity. *Multidiscip Model Mater Structures*. 2019; 15: 686-698.
[8] Megahed AM. Williamson fluid flow due to a nonlinearly stretching sheet with viscous dissipation and thermal radiation. *J Egypt Math Soc*. 2019; 27:12.
[9] Reddy BSK, Rao KVSN, Vijaya RB. Soret and Dufour effects on MHD flow of viscoelastic fluid past an infinite vertical stretching sheet. *Heat Transfer*. 2020; 49: 2330–2343.
[10] Mandal IC, Mukhopadhyay S. Eyring–Powel fluid flow past a power-law stretching permeable sheet in a free stream moving with power-law velocity in the presence of convective boundary condition, *Int J Ambient Energy*. 2019. DOI: 10.1080/01430750.2019.1691651.
[11] Kudenatti RB, Misbah Noor-E. Hydrodynamic flow of non-Newtonian power-law fluid past a moving wedge or a stretching sheet: a unified computational approach. *Scientific Reports*. 2020; 10: 9445.
[12] Shateyi S, Muzara H. On the Numerical Analysis of Unsteady MHD Boundary Layer Flow of Williamson Fluid Over a Stretching Sheet and Heat and Mass Transfers. *Computation*. 2020; 8(2): 55.
[13] Ro¸sca, NC, Pop I. Hybrid Nanofluids Flows Determined by a Permeable Power-Law Stretching/Shrinking Sheet Modulated by Orthogonal Surface Shear. *Entropy*, 2021; 23: 813.
[14] Ibrahim W, Negera M. MHD slip flow of upper-convected Maxwell nanofluid over a stretching sheet with chemical reaction, *J Egypt Math Soc*. 2020; 28:7.

[15] Dey D, Mahanta B. Rheology of power law fluid flow around a stagnation point in porous medium with energy dissipation, *Lat Am Appl Res.* 2021; 51(4): 223-228.
[16] Kumar KG, Ramesh GK, Gireesha BJ, Gorla RSR. Characteristics of Joule heating and viscous dissipation on three-dimensional flow of Oldroyd B nanofluid with thermal radiation. Alexandria Engineering Journal 2018; 57: 2139–2149.
[17] Das UJ. MHD mixed convective slip flow of casson fluid over a porous inclined plate with joule heating, viscous dissipation and thermal radiation, *J Math Comput Sci.* 2021; 11(3): 3263-3275.
[18] Rasheed UH, AL-Zubaidi A, Islam S, Saleem S, Khan Z, Khan W. Effects of Joule Heating and Viscous Dissipation on Magnetohydrodynamic Boundary Layer Flow of Jeffrey Nanofluid Over a Vertically Stretching Cylinder. *Coatings.* 2021; 11: 353.
[19] Forchheimer P. Wasserbewegung durch boden. *Zeitschrift des Vereins Deutscher Ingenieure*, 1901; 45: 1782–1788.
[20] Sadiq MA, Hayat T. Darcy-Forchheimer flow of magneto Maxwell liquid bounded by convectively heated sheet. *Results Phys*. 2016; 6: 884–890.
[21] Seth G, Tripathi R, Rashidi MM. Hydromagnetic natural convection flow in a non-Darcy medium with Soret and Dufour effects past an inclined stretching sheet. *J Porous Media*. 2017; 20: 941–960.
[22] Rasool G, Shafiq A, Khalique CM, Zhang T. Magnetohydrodynamic Darcy-Forchheimer nanofluid flow over a nonlinear stretching sheet. *Phys Scr*. 2019; 94: 105221.
[23] Misra SR, Baag S, Dash GC, Acharya MR. Numerical approach to MHD flow of power-law fluid on a stretching sheet with non-uniform heat source, *Nonlinear Eng*. 2020; 9: 81-93.
[24] Hayat T, Haider F, Alsaedi A. Darcy-Forchheimer flow with nonlinear mixed convection. *Appl Math Mech* (*English Edition*), 2020; 41(11): 1685–1696.
[25] Saeed A, Kumam P, Gul T, Alghamdi W, Kumam W, Khan A. Darcy–Forchheimer couple stress hybrid nanofluids flow with variable fluid properties, *Sci Rep*. 2021; 11:19612.
[26] Ullah B, Wahab HA, Khan U. Heat transfer investigation in Darcy-Forchheimer model by using nanoparticles, *Waves in Random and Complex Media*, 2022; DOI: 10.1080/17455030.2022.2048125.